LHC Electroweak Working Group

Jets and EW Bosons Subgroup Meeting – 20 April 2020

F Hautmann

The transverse momentum spectrum of low mass Drell-Yan production at next-to-leading order in the parton branching method

[based on A Bermudez et al, arXiv:2001.06488]

- The Parton Branching (PB) method
- Drell-Yan production at the LHC
- Drell-Yan in lower energy experiments

Parton Branching (PB) approach to TMDs

- The evolution of TMD distributions has been recently formulated in a parton branching formalism:

Jung, Lelek, Radescu, Zlebcik & H, "Collinear and TMD quark and gluon densities from parton branching", JHEP 1801 (2018) 070

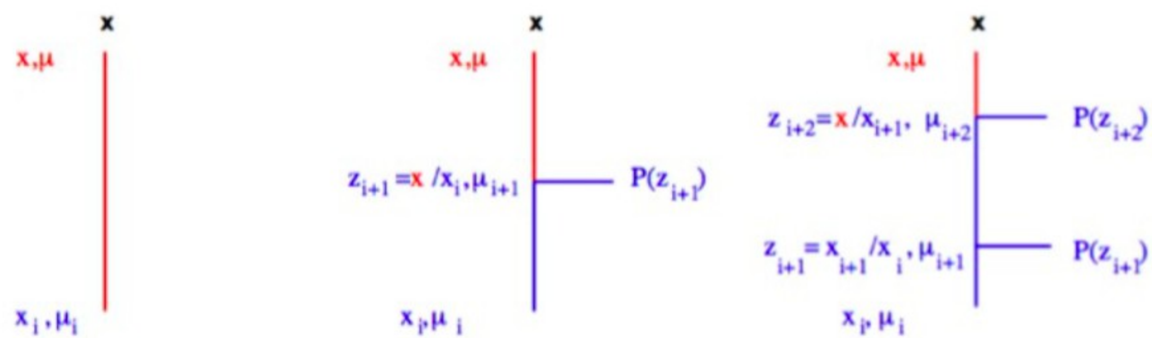

PB evolution equation motivated by

– applicability over large kinematic range from low to high transverse momenta

– applicability to exclusive final states and Monte Carlo event generators

- connection with DGLAP evolution of collinear parton distributions

PB evolution equation

$$\widetilde{A}_a\left(x,\boldsymbol{k},\mu^2\right)=\Delta_a\left(\mu^2,\mu_0^2\right)\widetilde{A}_a\left(x,\boldsymbol{k},\mu_0^2\right)+\sum_b\int\frac{\mathrm{d}^2\boldsymbol{\mu}'}{\pi\mu'^2}\Theta\left(\mu^2-\mu'^2\right)\Theta\left(\mu'^2-\mu_0^2\right)$$

$$\times\quad\int_x^1\mathrm{d}z\;\Theta\left(z_M(\mu')-z\right)\frac{\Delta_a\left(\mu^2,\mu_0^2\right)}{\Delta_a\left(\mu'^2,\mu_0^2\right)}P_{ab}^R\left(z,\alpha_s(b(z)^2\mu'^2)\right)\widetilde{A}_b\left(\frac{x}{z},\boldsymbol{k}+a(z)\boldsymbol{\mu}',\mu'^2\right)$$

$z_M(\mu')=1-q_0/\mu'$ $\qquad b(z)=1-z$ $\qquad a(z)=1-z$

NB: angular ordering

- solvable by iterative MC technique

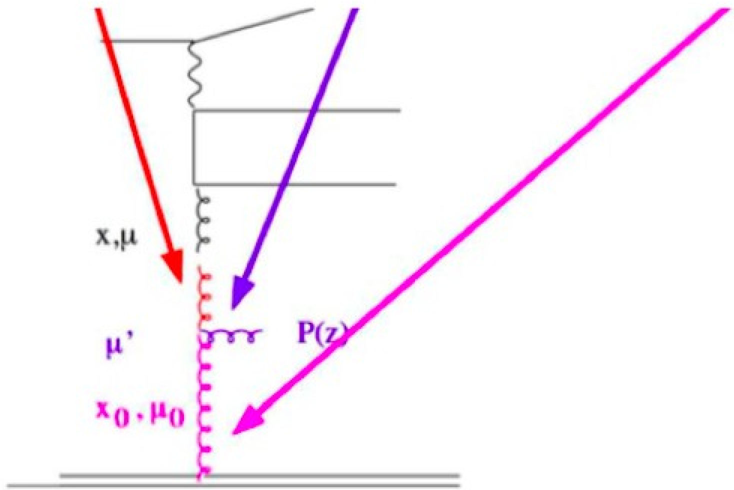

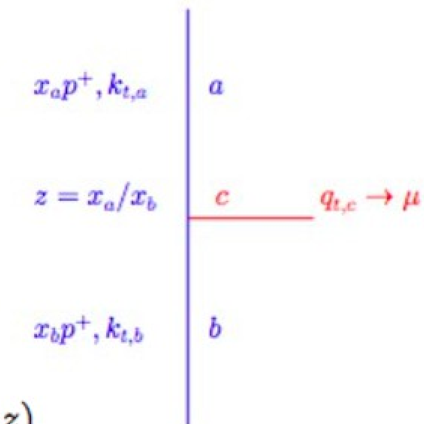

$\mu=|\mathbf{q}_c|/(1-z)$

where

$$\Delta_a(\mu^2,\mu_0^2)=\exp\left[-\sum_b\int_{\mu_0^2}^{\mu^2}\frac{\mathrm{d}\mu'^2}{\mu'^2}\int_0^1\mathrm{d}z\;\Theta\left(z_M(\mu')-z\right)\;z\;P_{ba}^R\left(z,\alpha_s\left(b(z)^2\mu'^2\right)\right)\right],\qquad P_{ba}^{(R)}(\alpha_s,z)=\delta_{ba}k_b(\alpha_s)\,\frac{1}{1-z}+R_{ba}(\alpha_s,z)$$

$$k_b(\alpha_s)=\sum_{n=1}^{\infty}\left(\frac{\alpha_s}{2\pi}\right)^n k_b^{(n-1)},\quad R_{ba}(\alpha_s,z)=\sum_{n=1}^{\infty}\left(\frac{\alpha_s}{2\pi}\right)^n R_{ba}^{(n-1)}(z)$$

Integrated PB-TMD with angular ordering:

$$\widetilde{f}_a(x,\mu^2) = \Delta_a(\mu^2,\mu_0^2)\widetilde{f}_a(x,\mu_0^2) + \sum_b \int_{\mu_0^2}^{\mu^2} \frac{d\mu'^2}{\mu'^2} \int_x^1 dz$$

$$\times \quad \Theta(1 - q_0/\mu' - z)\, \frac{\Delta_a(\mu^2,\mu_0^2)}{\Delta_a(\mu'^2,\mu_0^2)}\, P_{ab}^R\left(z, \alpha_s\left((1-z)^2\mu'^2\right)\right) \widetilde{f}_b\left(\frac{x}{z},\mu'^2\right)$$

- coincide with CMW result for coherent branching

[Catani-Marchesini-Webber, Nucl. Phys. B349 (1991) 635;

Marchesini-Webber, Nucl. Phys. B310 (1988) 461.]

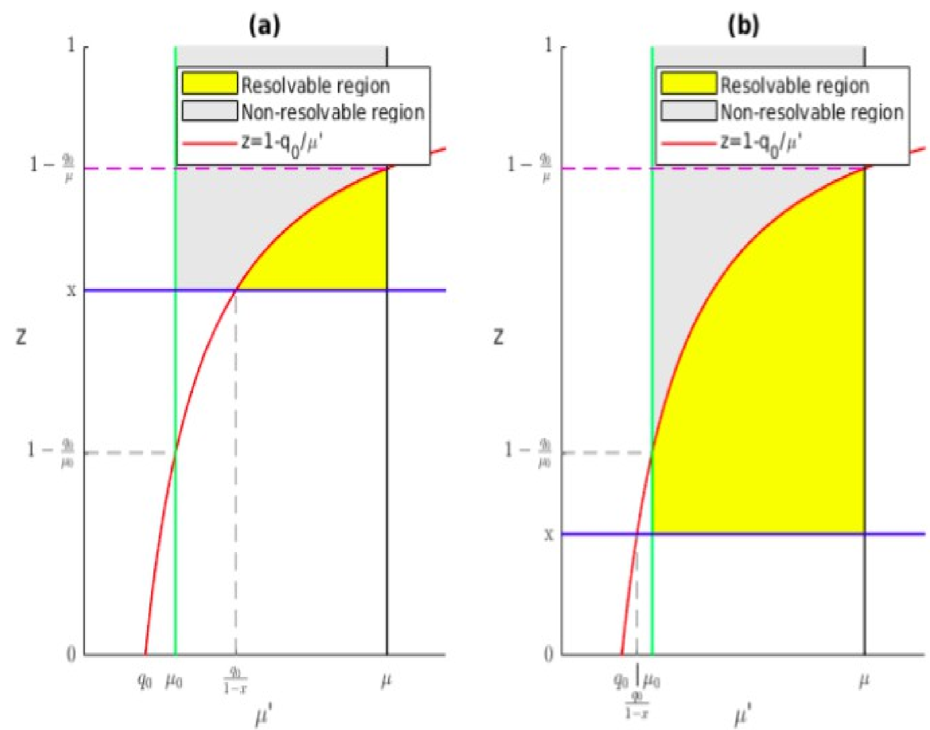

Figure 2: The angular ordering condition $z_M(\mu') = 1 - q_0/\mu'$ with the resolvable and non-resolvable emission regions in the (μ', z) plane: a) the case $1 > x \geq 1 - q_0/\mu_0$; b) the case $1 - q_0/\mu_0 > x > 0$.

Keersmaekers, Lelek, van Kampen & H, Nucl. Phys. B 949 (2019) 114795 [arXiv:1908.08524 [hep-ph]]

Integrated PB-TMD with $z_M \to 1$ and $\alpha_s \to \alpha_s(\mu'^2)$ ---> collinear PDFs

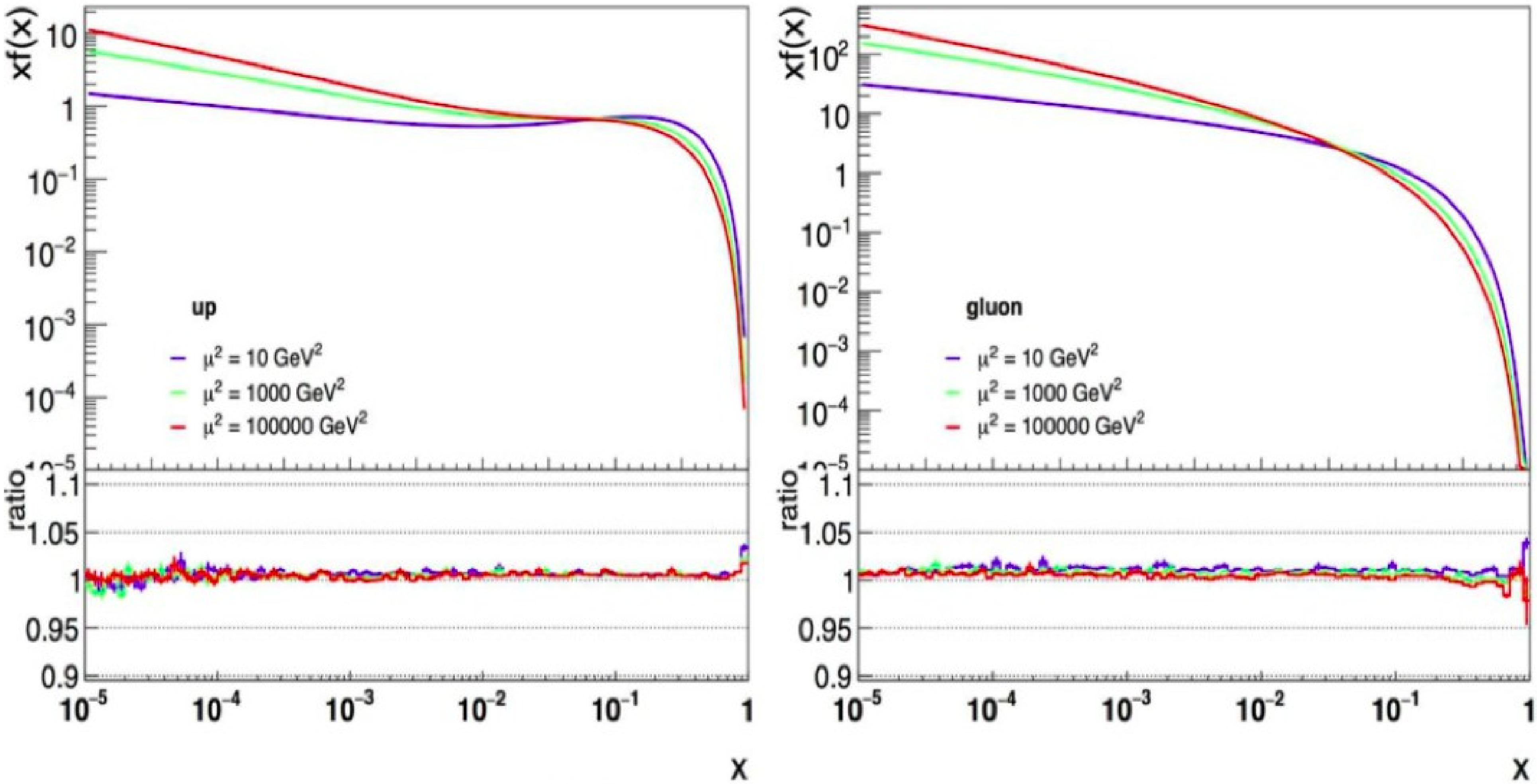

Very good agreement at NLO over all x and mu.
NB: the same approach is designed to work at NNLO.

- Equivalent to DGLAP evolution equation for zM → 1

3D Imaging and Monte Carlo

- **Parton Branching evolution**
  - start from hadron side and evolve from small to large scale μ^2

$$\Delta_s = \exp\left(-\int^{z_M} dz \int_{\mu_0^2}^{\mu^2} \frac{\alpha_s}{2\pi}\frac{d\mu'^2}{\mu'^2} P(z)\right)$$

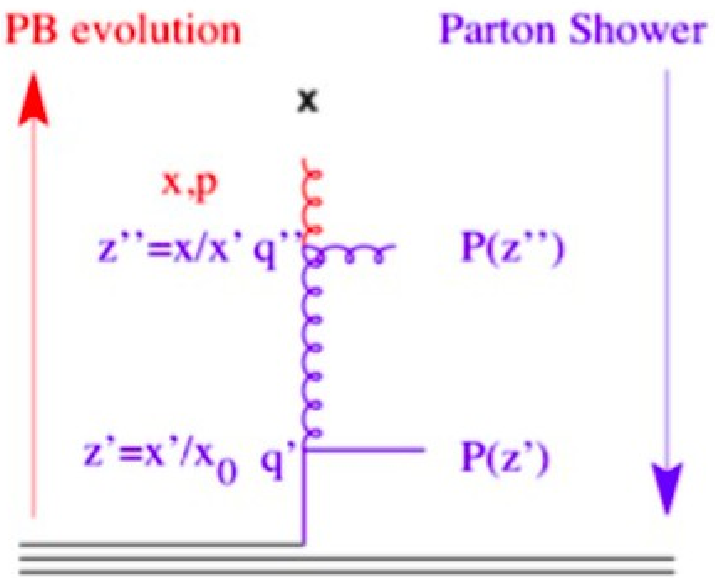

- **Parton Shower**
  - backward evolution from hard scale μ^2 to hadron scale μ^2_0 (for efficiency reasons)

$$\Delta_s = \exp\left(-\int^{z_M} dz \int_{\mu_0^2}^{\mu^2} \frac{\alpha_s}{2\pi}\frac{d\mu'^2}{\mu'^2} P(z) \frac{\frac{x}{z}\mathcal{A}\left(\frac{x}{z}, k'_\perp, \mu'\right)}{x\mathcal{A}(x, k_\perp, \mu')}\right)$$

➔ in backward evolution, parton density (TMD) imposed further constraint !

APPLICATIONS to DIS and DY

PB method in xFitter

TMD distributions from fits to precision inclusive-DIS data from HERA using the open source QCD platform xFitter [*S. Alekhin et al., E. Phys. J. C 75 (2014) 304*]

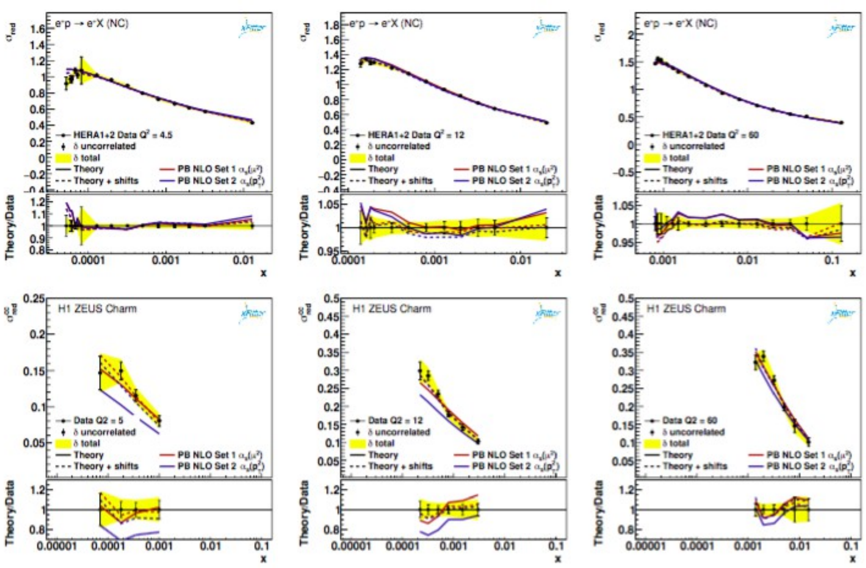

Figure 5: Measurement of the reduced cross section obtained at HERA compared to predictions using Set 1 and Set 2. Upper row: inclusive DIS cross section [11], lower row: inclusive charm production [38]. The dashed lines include the systematic shifts in the theory prediction.

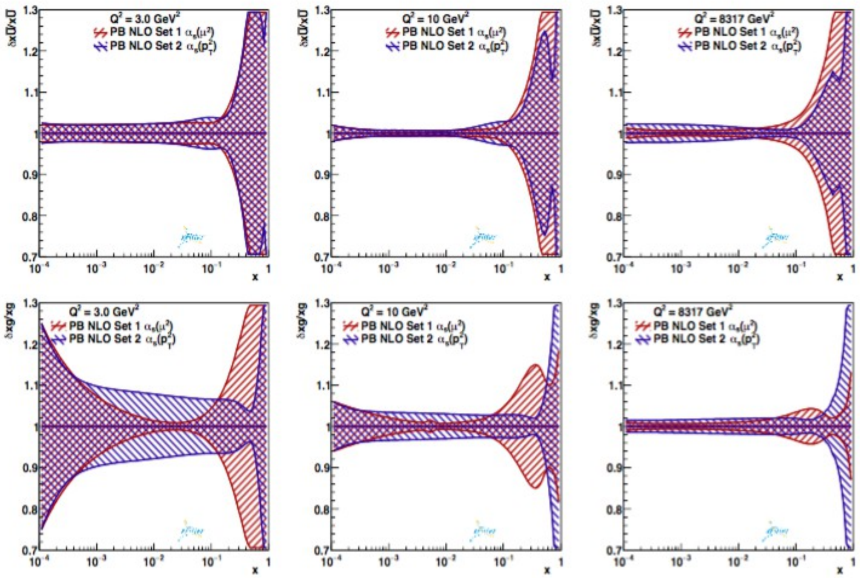

Figure 4: Total uncertainties (experimental and model uncertainties) for the two different sets at different values of the evolution scale μ^2.

A. Bermudez et al., Phys. Rev. D99 (2019) 074008

- NLO determination of TMDs including uncertainties

Z-boson DY production at the LHC:
TMDs fitted to inclusive DIS + NLO DY calculation

A Bermudez et al, PRD 100 (2019) 074027
[arXiv:1906.00919]

- Use MadGraph5_aMC-at-NLO
- Apply PB-TMD
- Set matching scale mu_m (kT < mu_m)

ATLAS 8 TeV data [E. Phys. J. C76 (2016) 291]

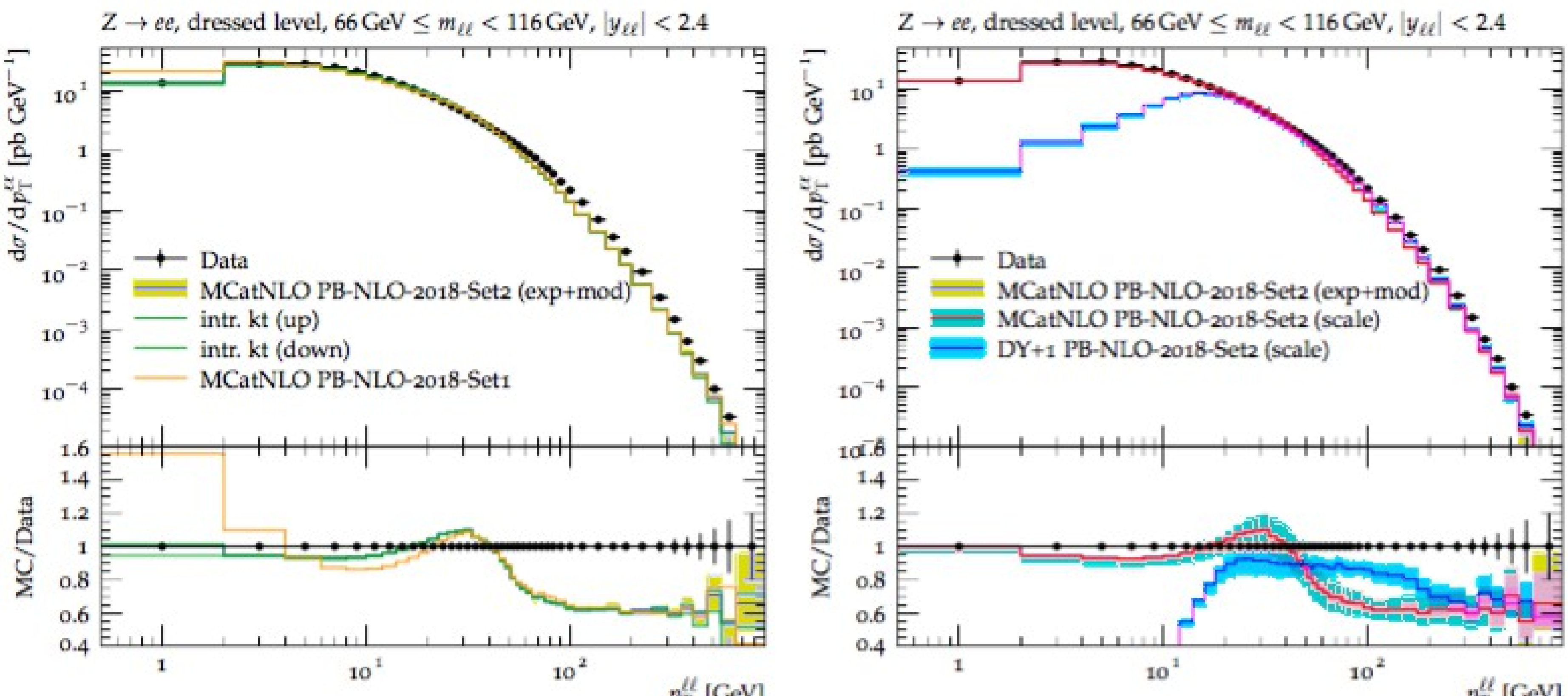

- Theoretical uncertainties dominated by scale dependences; TMD uncertainties moderate
- Low-pT spectrum sensitive to angular ordering (PB-TMD Set 2)
- Missing higher orders at high pT: see DY + 1 jet contribution

Z-boson DY production at the LHC:
TMDs fitted to inclusive DIS + NLO DY calculation

A Bermudez et al, PRD 100 (2019) 074027
[arXiv:1906.00919]

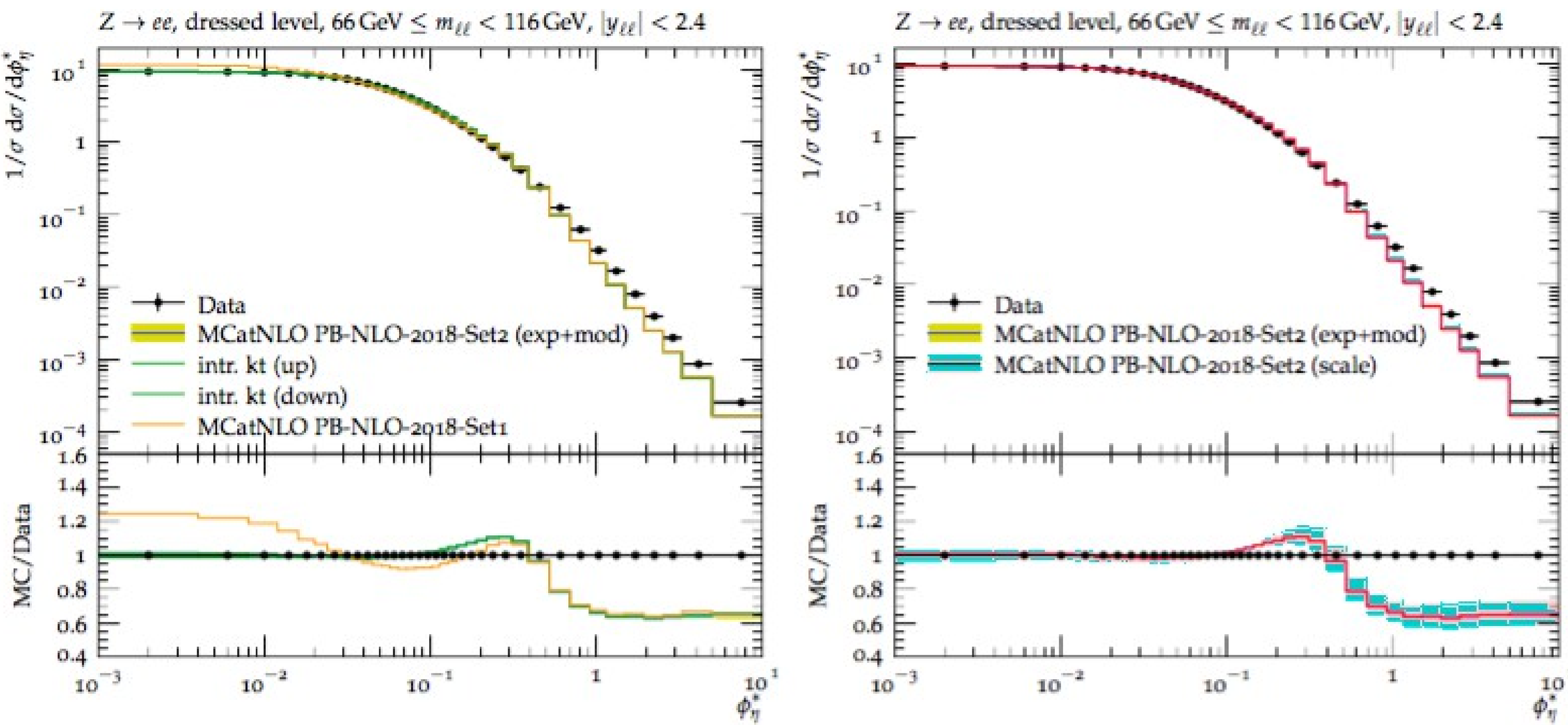

ATLAS 8 TeV data [E. Phys. J. C76 (2016) 291]

Comment on matching of low qT and high qT

CSS-TMD:

$$\frac{d\sigma}{dq_T dQ^2} = W[\mathcal{F}] + Y[f] + \mathcal{O}\left(\frac{\Lambda^2_{\rm QCD}}{Q^2}\right)$$

PB-TMD:

$$\sigma[w] = \sum_{\text{final states } X} w(X) \, \mathrm{PB} \otimes \hat{H}$$

$$\mathrm{PB} \otimes \left[H^{(\mathrm{LO})} + \alpha_s \left(H^{(\mathrm{NLO})} - \mathrm{PB}(1) \otimes H^{(\mathrm{LO})}\right)\right]$$

[see Collins & H, JHEP 0103 (2001) 016 [hep-ph/0009286]]

Can we go to low masses and low energies?

Low energy case:

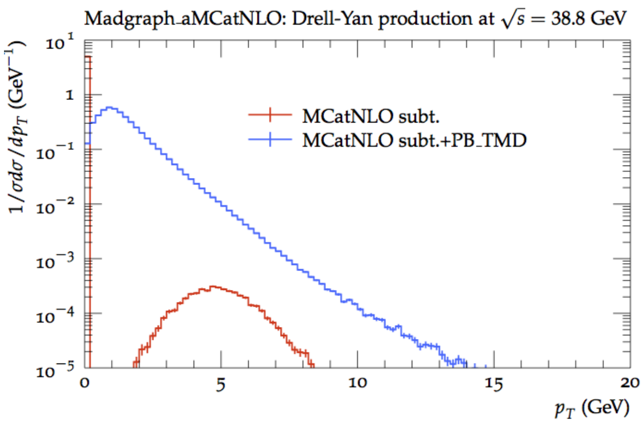

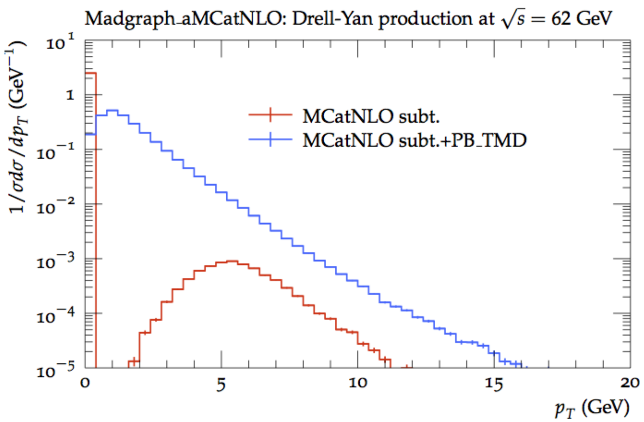

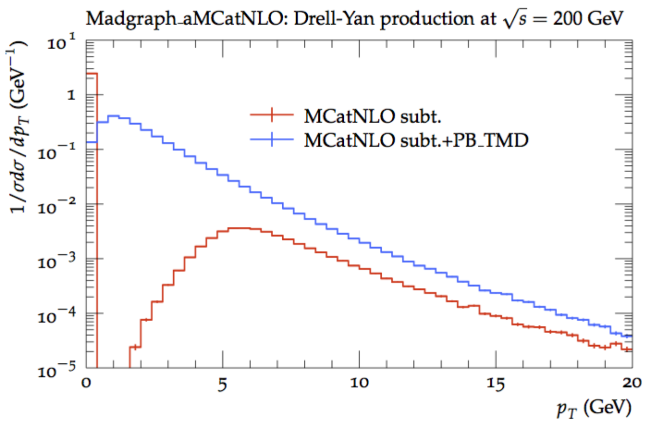

- Interplay of TMD and collinear contributions works quite differently in the two cases
- - > for pT < < M, TMD effects are significant for both LHC and low-energy cases
- - > for pT ~ M, multiparton radiation from TMD evolution is small effect at the LHC but significant in low-energy case!

LHC case:

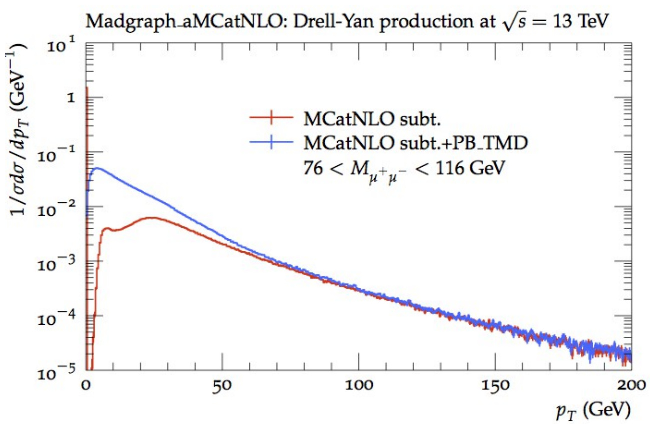

DY production at low energy: mass spectra

A Bermudez et al, arXiv:2001.06488

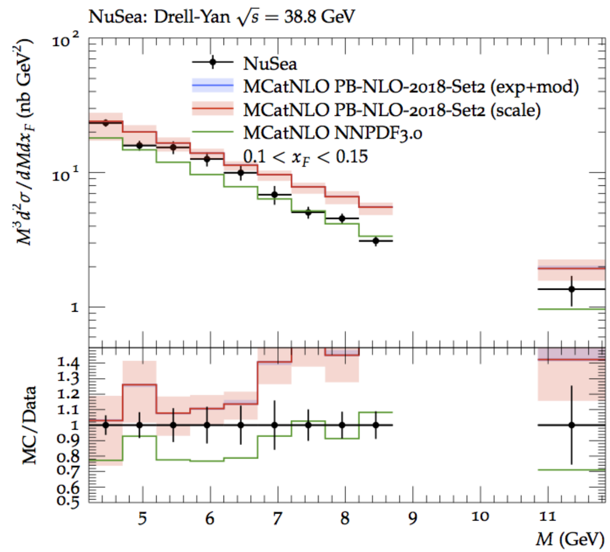

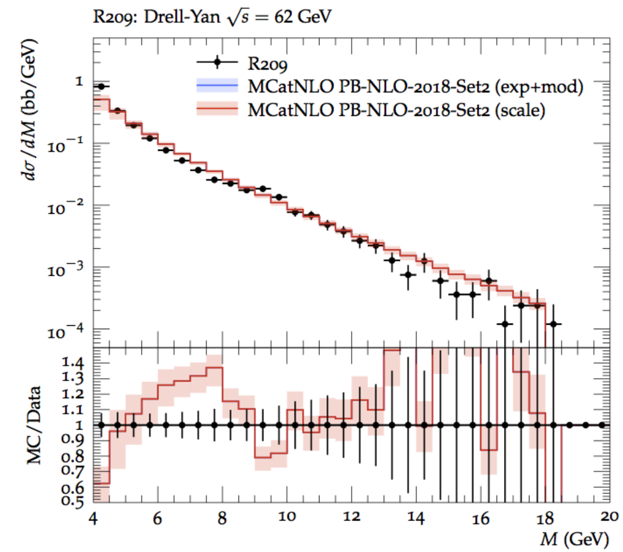

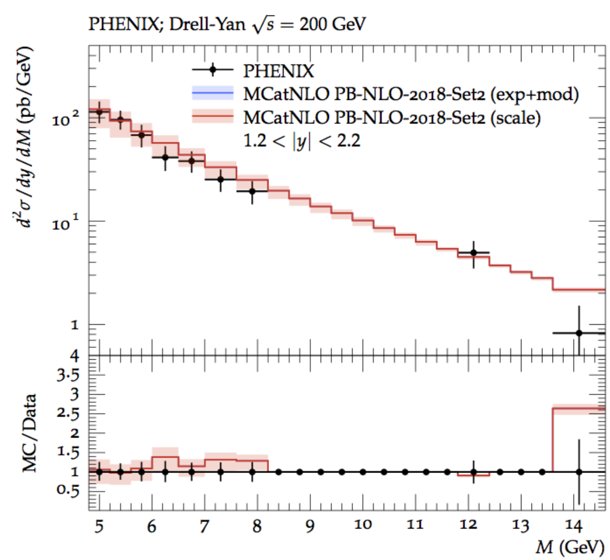

- mass spectra are generally well described by PB TMDs + NLO
- for region of highest masses at lowest energy (NuSea), large-x region is entered where HERA data poorly constrain parton distributions
  - > use NNPDF global fit
- region of lowest masses < 6 GeV at NuSea well described

DY production at low energy: transverse momentum spectra

A Bermudez et al, arXiv:2001.06488

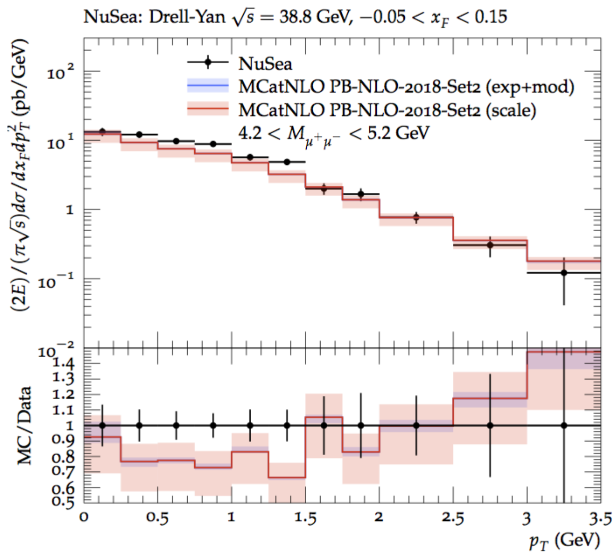

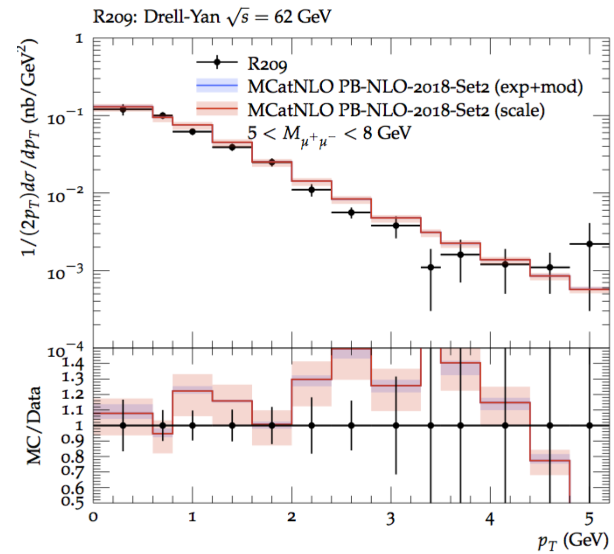

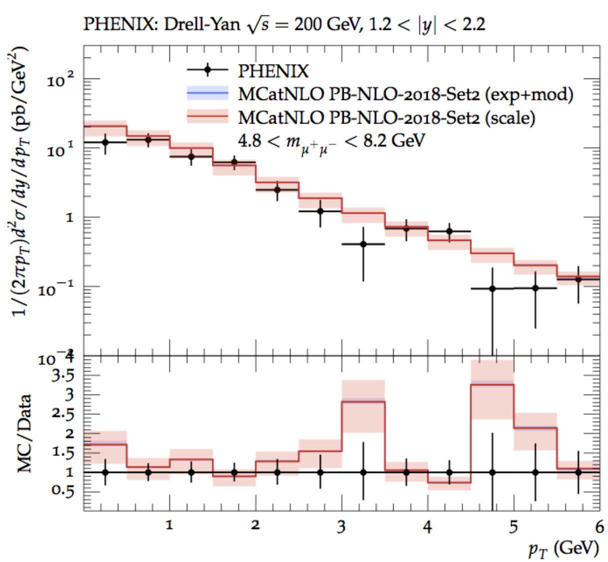

- Inclusion of multiparton radiation by PB TMD evolution is essential to describe pT spectra at low energy all the way up to pT ~ M

$\chi^2/ndf = 1.08, 1.27, 1.04$ for NuSea, R209 and PHENIX, respectively

(for 13 TeV CMS data: $\chi^2/ndf = 0.8$ for $p_T < 80$ GeV)

- Much larger effects from intrinsic kT at low energy

DY production at low energy: intrinsic kT

A Bermudez et al, arXiv:2001.06488

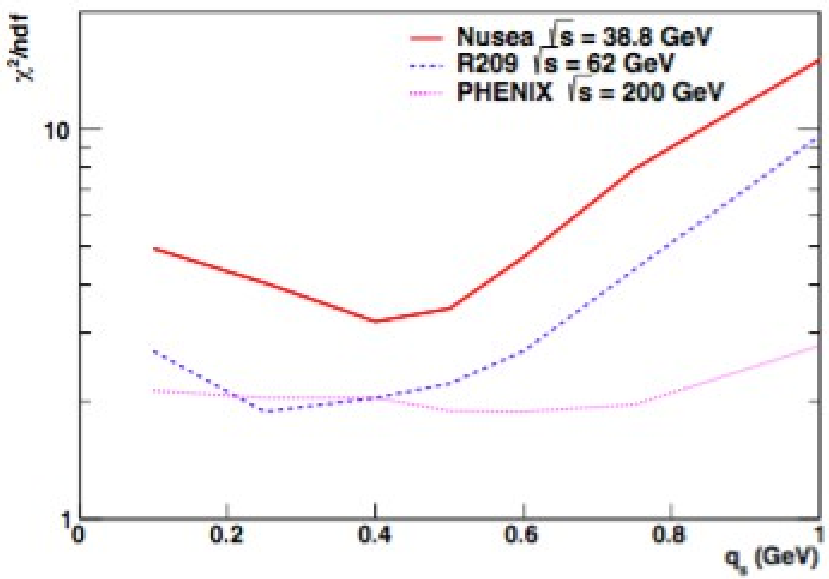

Figure 8: The χ^2/ndf as a function of the width of the intrinsic transverse momentum distribution, obtained from a comparison of the measurements (NuSea [42, 43], R209 [41], PHENIX [40]) with a prediction at NLO using PB-TMDs. For the theory prediction only the central value is taken, but no uncertainty from scale variation is included.

Final remarks

- It has been observed in the literature (see e.g. Bacchetta et al, Phys Rev D100 (2019) 014018 [arXiv:1901.06916]) that NLO collinear calculations are not able to describe DY pT spectra at fixed-target experiments in the region pT ~ M.

- This is consistent with our findings on the interplay of TMD and collinear terms in the LHC and fixed-target kinematics.

- In contrast to the above observation in the literature, we find that a good description of the DY pT spectra is achieved, including the region pT ~ M at fixed target, by matching PB TMDs with NLO.

- We find that at low energies and low masses multiparton radiation from TMD evolution is relevant throughout the region pT ~ M. This is different from the LHC case.

- Our results imply that nonperturbative TMD information (such as intrinsic kT) can usefully be extracted from low-energy DY measurements.

EXTRA SLIDES

Z-boson DY production at 13 TeV

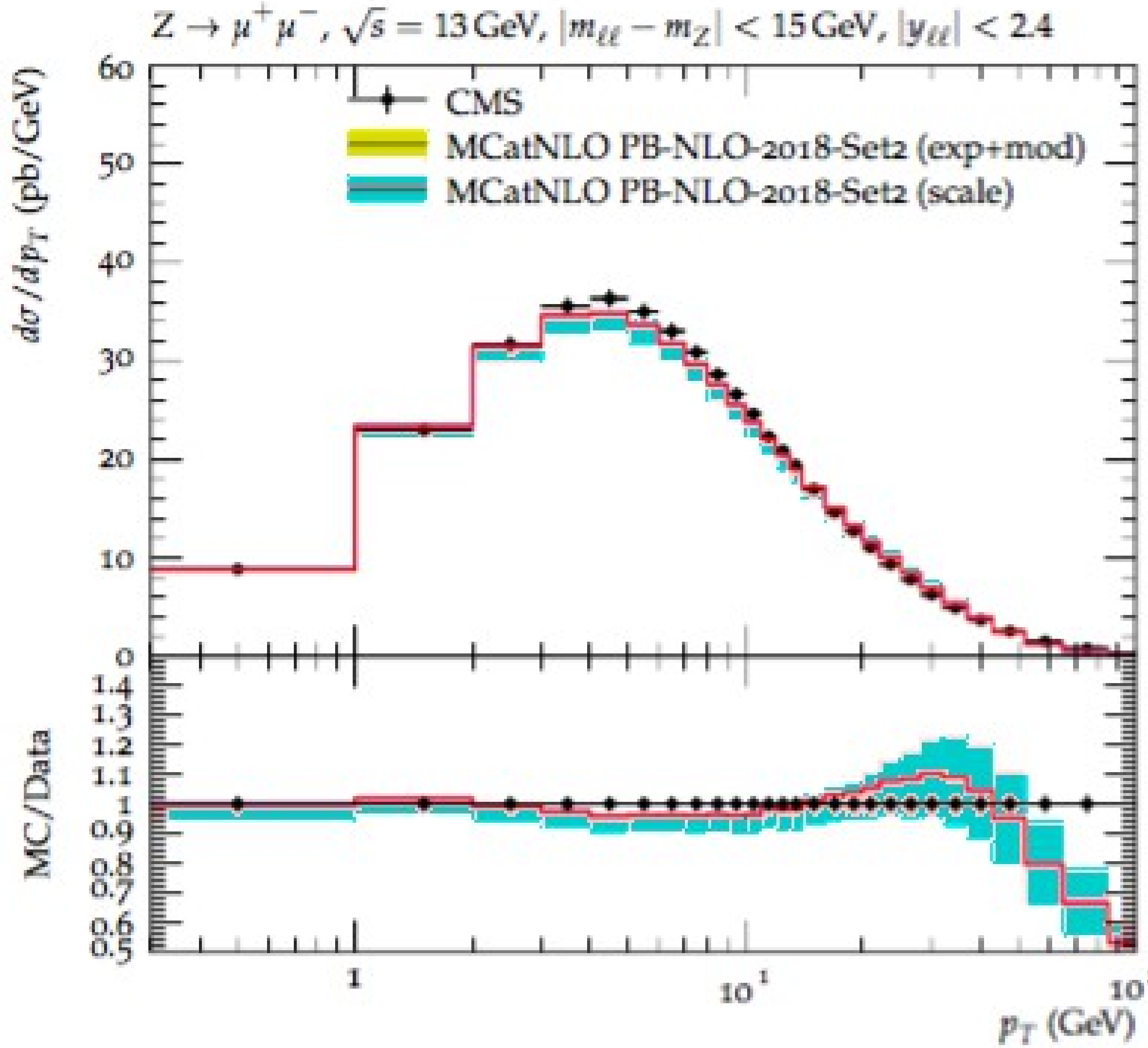

The drop in the prediction at large transverse momenta comes from missing higher order contributions in the hard process calculation, as discussed in Ref. [36].

Transverse momentum dependent (TMD) parton distribution functions

- Nonperturbative correlation functions of parton fields
  needed in QCD factorization theorems
  to sum classes of logarithmic radiative corrections
  to all orders in the strong coupling alpha_s

EXAMPLES:

low q_T : $q_T \ll Q$

$\alpha_s^n \ln^m Q/q_T$

low-qT factorization

high $\sqrt{s}$: $\sqrt{s} \gg M$

$(\alpha_s \ln \sqrt{s}/M)^n$

high-energy factorization

- See e.g. R. Angeles-Martinez et al., “Transverse momentum dependent (TMD) parton distribution functions: status and prospects”, Acta Phys. Polon. B46 (2015) 2501

Dynamical soft-gluon resolution scale

- The resolution parameter zM separates hard ("resolvable") color radiation *(yellow regions)* and soft ("non-resolvable") color radiation *(grey regions)*
- This separation depends on the branching scale for evolution. The boundary between "hard" and "soft" varies with mu *(red curve)*.
- Angular-ordered evolution requires that zM varies with mu as

  zM = 1 – q0 / mu.
- q0 has the meaning of minimum transverse momentum with which any emitted parton can be resolved.

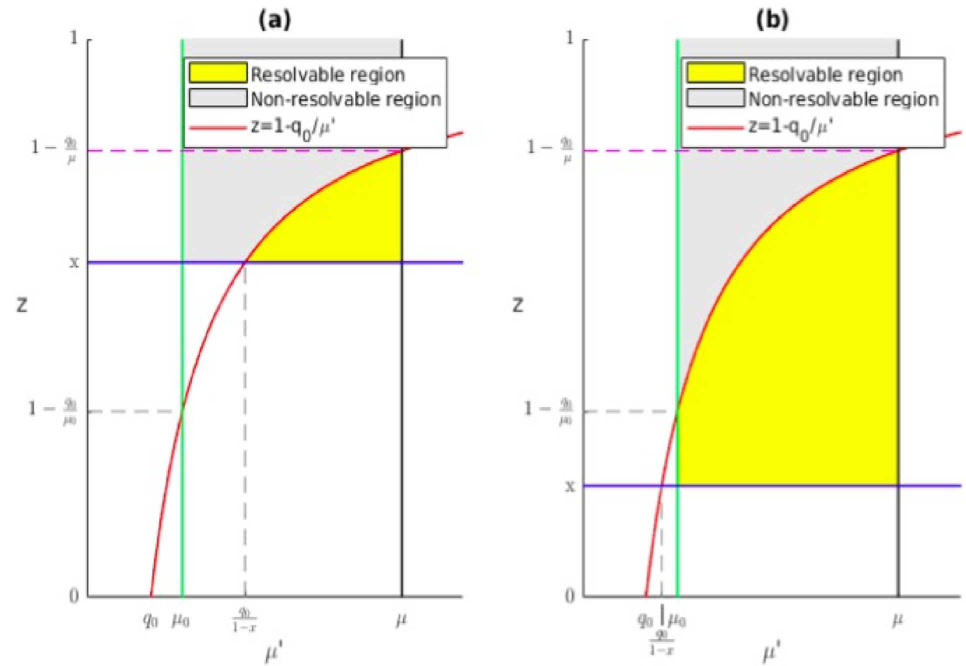

Figure 2: The angular ordering condition $z_M(\mu') = 1 - q_0/\mu'$ with the resolvable and non-resolvabl emission regions in the (μ', z) plane: a) the case $1 > x \geq 1 - q_0/\mu_0$; b) the case $1 - q_0/\mu_0 > x > 0$.

- For x < 1 – q0 / mu0: evolution down to mu0
- For x > 1 – q0 / mu0: evolution down to q0 / (1 – x)

Nucl. Phys. B 949 (2019) 114795

TMD distribution functions from precision DIS data fits

- NLO determination of TMDs including uncertainties

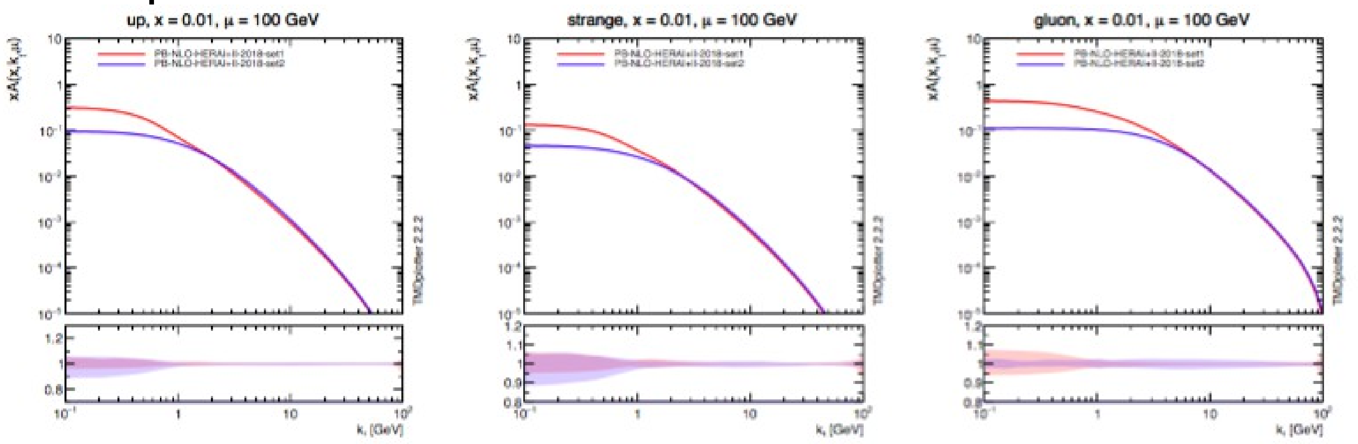

Figure 2: TMD parton distributions for up, strange and gluon (PB-NLO-2018-Set1 and PB-NLO-2018-Set 2) as a function of k_t at $\mu = 100$ GeVand $x = 0.01$.

A. Bermudez et al., Phys. Rev. D99 (2019) 074008

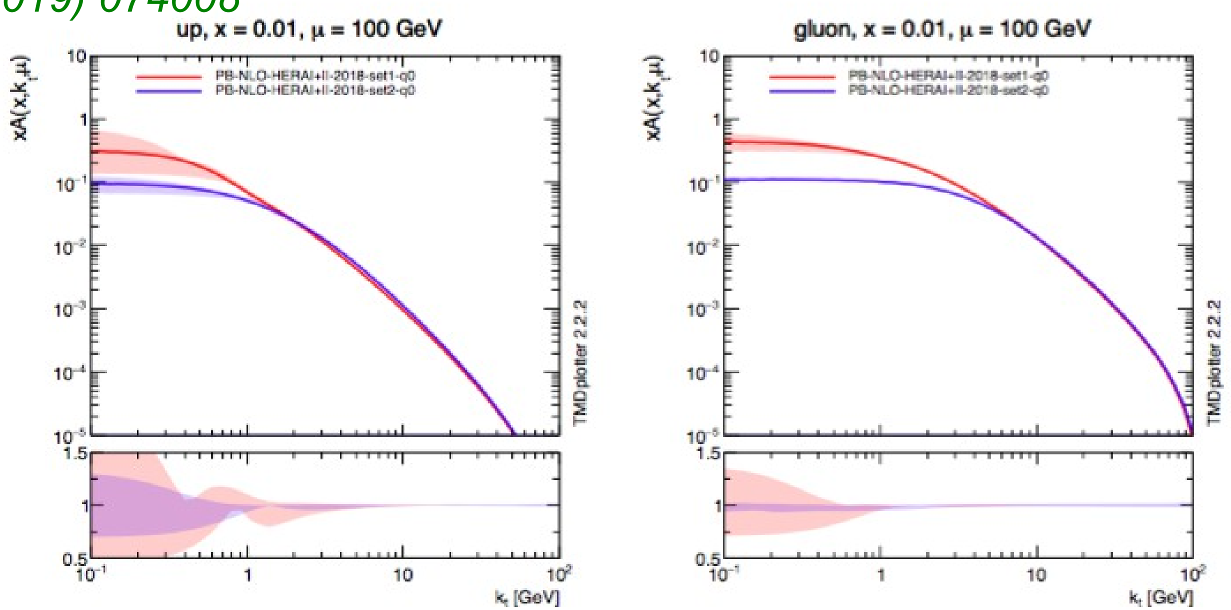

- can improve sensitivity at low kT by precise semi-inclusive DIS measurements at future ep/eA colliders

Figure 3: TMD parton distributions for up-quark and gluon (PB-NLO-2018-Set1 and PB-NLO-2018-Set 2) as a function of k_t at $\mu = 100$ GeVand $x = 0.01$ with a variation of the mean of the intrinsic k_t distribution.